

Facies analysis and depositional environment study of the mixed carbonate–evaporite Asmari Formation (Oligo-Miocene) in the sequence stratigraphic framework, NW Zagros, Iran

Mehdi Daraei · Abdolhossein Amini ·
Morteza Ansari

Accepted: 22 June 2014 / Published online: 25 July 2014
© Springer-Verlag Berlin Heidelberg 2014

Abstract The carbonate–evaporite mixed Asmari Formation was investigated on the three representative outcrops (these of Zarrin-abad, Abhar, and Darreh-shahr, corresponding to three sections) of the Lurestan Zone in NW Zagros, where the sedimentary facies of the Asmari Formation shows significant differences to those in other parts of Zagros. In the light of study results from the field observation and laboratory measurements, 16 facies have been recognized and differentiated, which are grouped into 5 facies associations, representing 6 sub-environments on a carbonate ramp. The sub-environments include peritidal area, lagoon, platform margin high-energy belts, middle ramp, outer ramp and evaporitic saltern. The evaporitic saltern points to such a condition, during which there occurred periodic change from carbonate to evaporitic settings. The alternation of carbonate with evaporitic settings appeared on a carbonate ramp connected with a hydrographically isolated intrashelf basin. The development of evaporite-dominated deposits of the Kalhur Member of Asmari Formation is related to the restriction of the basin during sea-level falls. This restriction led to succeeding evaporation of seawater and precipitation of evaporites. In times of sea-level rising, the basin was well reconnected to open ocean and thus the carbonate factory was reestablished over the basin. From sequence stratigraphic points of view, the formation is composed of two second-order regressive sequences, representing transitional conditions from deep-marine facies underlying Pabdeh Formation to shallow evaporitic facies overlying Gachsaran Formation. Each sequence is composed of a unit

of evaporites at bottom displaying a falling-stage systems tract followed by thick carbonate strata, representing transgressive and highstand systems tracts. It is obvious that the major relative sea-level fall of the first second-order sequence was recorded by the facies development of the upper Kalhur gypsum of the Asmari Formation in the Zarrin-abad section, and there developed the paleokarst facies located at the sequence boundary in the Abhar, and Darreh-shahr sections.

Keywords Zagros · Iran · Asmari Formation · Facies analysis · Intrashelf basin

Introduction

The Oligo-Miocene Asmari Formation in the Zagros foreland basin, SW Iran, contains the most prolific oil reserve of Iran (Koop and Stoneley 1982; James and Wynd 1965), which is estimated to hold more than 90 % of the recoverable oil of Iran and Iraq (Ghazban 2007). The major source rocks of the oil are under debate and are estimated to be the underlying Lower Cretaceous strata (Kazhdumi Formation) (Ala 1982), the Upper Cretaceous and Eocene marls (Gurpi and Pabdeh formations) (Falcon 1958) or the rocks of the Asmari Formation itself (Kashfi 1984). It is presumed that the oil generation and migration were in the Post-Eocene and in the Recent, respectively (Ala 1982). The occurrence of the oil in this formation is principally controlled by fractures (referred to as fractured reservoirs by Ahr 2008), and neither by sedimentary nor by diagenetic factors (McQuillan 1974; Ala 1982; Motiei 1993).

This formation occurs in most zones of NW–SE trending Zagros orogenic belt (dominantly as subcrops in SE and outcrops in NW Zagros). The formation shows

M. Daraei (✉) · A. Amini · M. Ansari
School of Geology, College of Science, University of Tehran,
Tehran, Iran
e-mail: DaraeiMehdi@gmail.com

significant variation in thickness (from about 200 to 500 m) and facies constitution (Motiei 1993). It is characterized by dominant carbonate facies in most parts of Zagros (Fig. 1a), siliciclastic-carbonate mixed facies in central to southern parts of the Zagros belt (known as Dezful Embayment; Fig. 2) and carbonate-evaporite mixed facies in the northwestern part of Zagros (Lurestan; Fig. 2). Consequently, two distinct members are distinguished in the carbonate-dominated facies belt of the Asmari Formation known as Ahwaz (sandstone) and Kalhur (evaporite) members (James and Wynd 1965). The Ahwaz Sandstone Member is dominantly observed in the north Dezful Embayment, and is more common in the Ahwaz, Marun, Mansuri and Cheshmeh-Khosh oil fields. The Kalhur Evaporite Member is dominantly observed in the Lurestan zone (Figs. 1a, 2a).

It is reported that the Asmari Formation conformably overlies the Paleocene to Oligocene Pabdeh Formation in most places, but overlies the Jahrom Formation in the Fars region and Pabdeh Formation in the NW Lurestan (Fig. 1) (e.g., Wynd 1965; Adams and Bourgeois 1967). The formation is overlain by the Middle to Upper Miocene Gachsaran Formation in most places (Fig. 1).

According to the biostratigraphic analysis, the formation is subdivided into lower (Oligocene), middle (Aquitainian), and upper (Burdigalian) parts (Adams and Bourgeois 1967; Fig. 1b). It is believed that the formation is Early Miocene (Aquitainian and Burdigalian) in age where the Kalhur Member is present (Bahrami 2000; Nayebi 2003).

Due to the significant reservoir potential of the formation, broad investigations have been made (e.g., Seyrafiyan and Mojikhalifeh 2005; Seyrafiyan 2000; Aqrawi et al. 2006; Vaziri-Moghaddam et al. 2006; Amirshahkarami et al. 2007; Ehrenberg et al. 2007; Mosadegh et al. 2009; Sadeghi et al. 2009; van Buchem et al. 2010). Characteristics and depositional environment of the formation have been studied; only the Lurestan zone dominated by evaporites is less studied so far. Different contributors argue whether the depositional environment of the evaporite facies in the Kalhur Member of the formation is related to sabkha settings (e.g., Seyrafiyan et al. 2007; IOR 2006) or to basinal settings (e.g., Thomas 1952; Wells 1967). This study aims firstly to investigate the facies characteristics of the formation in the northwest Lurestan, where significant exposures of the evaporite facies are observed and secondly to reconstruct the depositional condition of the

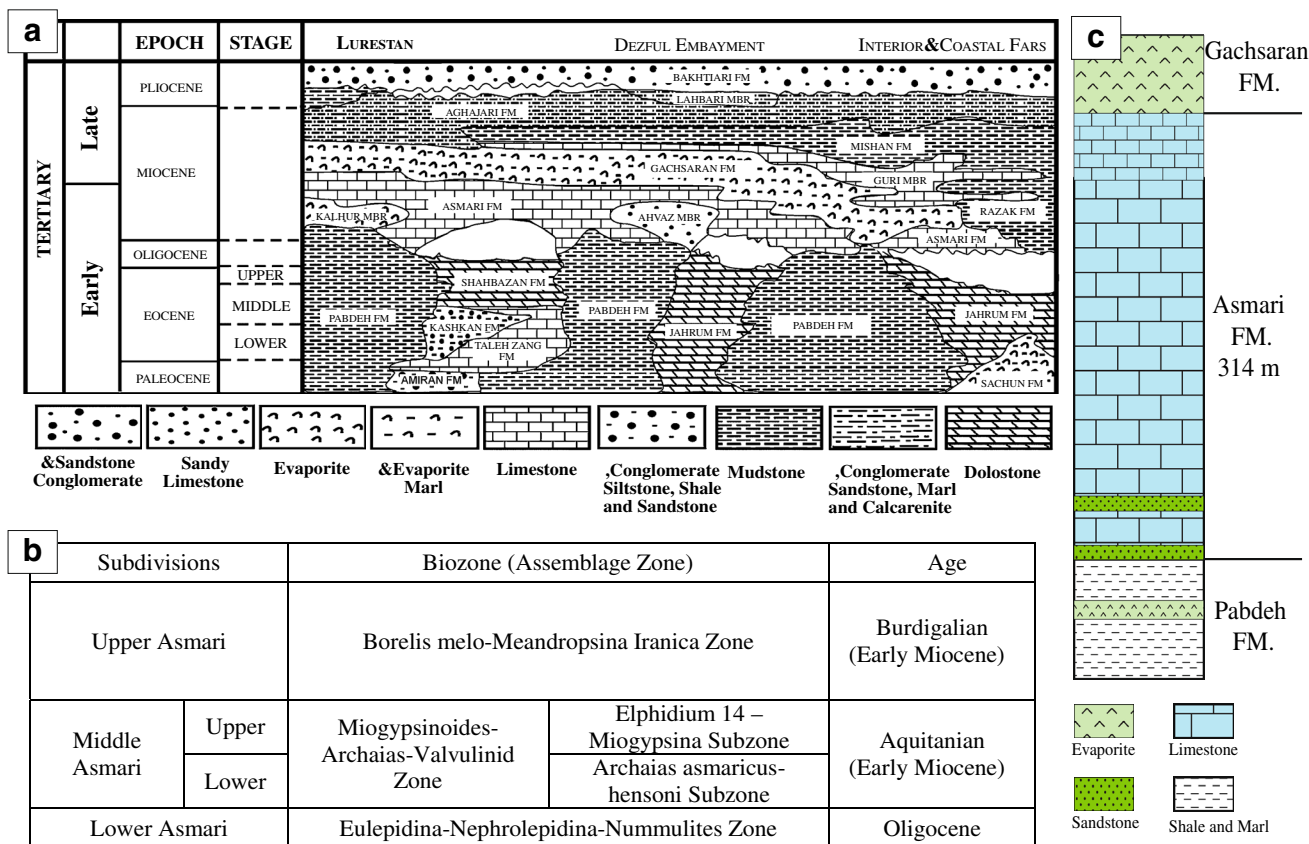


Fig. 1 a Stratigraphic position of the Asmari Formation and its distribution in the Zagros area (modified from Ala1982). b Subdivisions, biozones and age of the Asmari Formation (after Adams and Bourgeois 1967). c Type section of the Asmari Formation (after Richardson 1924)

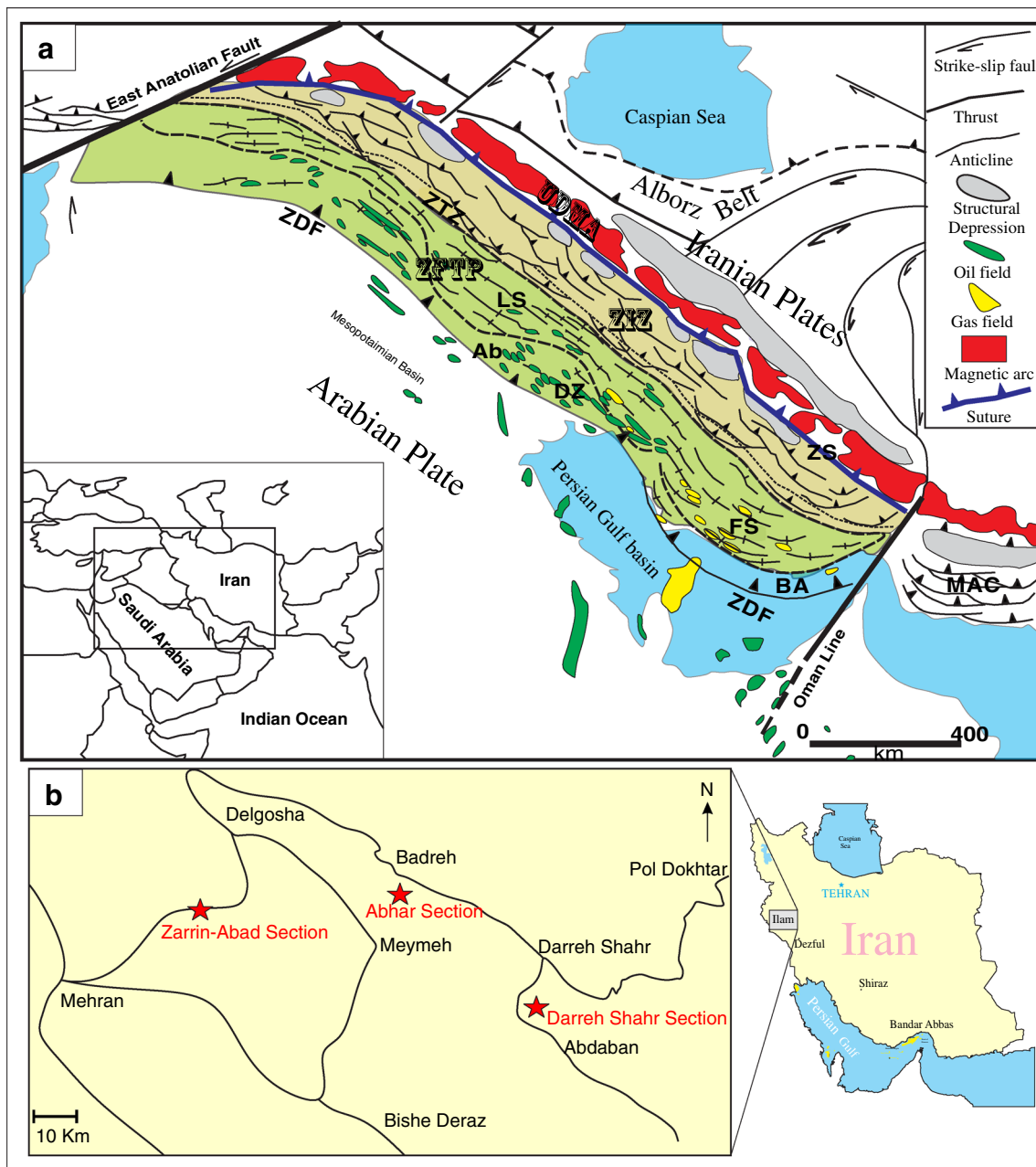


Fig. 2 **a** Geological setting of the Zagros belt in SW Iran and its neighboring zones and subdivisions. *DZ* Dezful Embayment, *FS* Fars zone, *LS* Lurestan zone, *IZ* Izeh zone, *Ab* Abadan Plain, *BA* Bandar-Abbas hinterland, *MAC* Makran accretionary complex, *UDMA*

Urumieh–Dokhtar magmatic assemblage, *ZDF* Zagros deformational front, *ZFTB* Zagros fold-thrust belt, *ZIZ* Zagros imbricated zone, *ZS* Zagros suture (modified from Alavi 2007). **b** Location map of the studied sections

formation. Variation of the depositional conditions of the formation in time and space is discussed in a sequence stratigraphic framework.

Geological setting

The NW–SE trending mountains of west/southwest Iran (Lurestan, Khuzestan and Fars regions) are parts of the

Alp–Himalayan orogenic belt, known as the Zagros belt/zone/range. The Zagros belt represents NE margin of the Arabian plate, in which discontinuous deposition occurred from the latest Precambrian to Late Miocene (e.g., Berberian and King 1981; Alavi 2004). The Zagros range is known as a product of the Neo-Tethyan closure, during which progressive folding, faulting and structural deformation of strata resulted in the formation of High Zagros (Zagros Imbricated Zone) and in the Simply Folded Zone

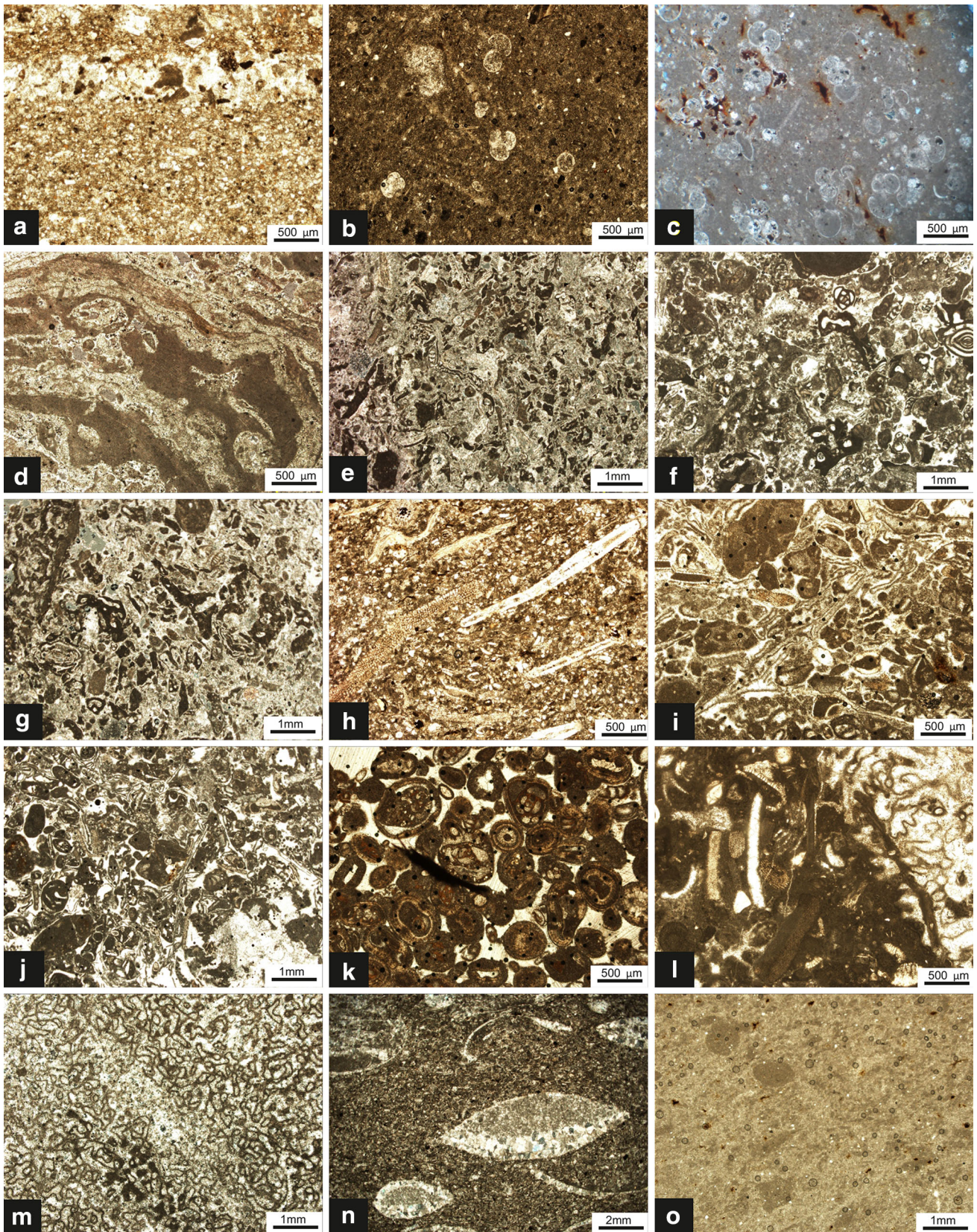


Fig. 3 Representative photomicrographs of some facies in the studied sections: **a** Bioclast hemipelagic packstone–grainstone (Facies A₁); mixing of shallow and deep-marine allochems is the characteristic. Scoured-based laminations are also seen. The facies represents storm action across the Asmari ramp. **b, c** Facies A₂: Planktonic foraminifera wackestone–packstone; planktonic foraminifera (mostly Globigerinidea) are the main allochem. **d–g** Coralline algae rudstone to packstone (Facies B₁); crustose and articulated coralline algae are the main constituent. This facies in the proximal mid-ramp contains large quantities of porcelaneous foraminifera, which are in decreasing order seaward. Rhodolitic fabrics become common seaward (**d**). **h** LBF wackestone (Facies B₂); Larger hyaline benthic foraminifera (here *Operculina spp.*) with/without coralline algae makes distal limit (oligophotic) of the mid-ramp. **i, j** Red algae foraminifera rudstone–grainstone; this facies makes seaward shoal of the ramp and is in transitional nature with Facies B₁. Intraclasts and cemented background point to high-energy setting. **k** Oolitic grainstone–packstone facies (C₂). **l** Bioclast rudstone to floatstone (C₃); bivalve, red algae and corals are the constituents. The facies points to coralgal patch-reef zone of the ramp where fair weather waves meet sea floor. **m** Coral boundstone (Facies C₄). **n** Mollusca wackestone–packstone (D₁). **o** Bioturbated peloidal wackestone–mudstone (D₂); bioturbation and peloids (mainly of Bahamite type) are the features

(Zagros Fold-Thrust Belt; Fig. 2a). The closure is related to the Arabian Plate subduction beneath the Central Iran Plate that was formed in the Late Cretaceous (Berberian and King 1981; Stocklin 1974; Takin 1972; Alavi 2004). Subsequently, the collisional mountain building that began in Middle Maastrichtian (about 68 Ma) has continued with variable intensity until the Recent (Alavi 2004). This collision led to the closure of the Neo-Tethys basin and the formation of *Zagros foreland basin* with a sedimentary record from the Late Cretaceous to the Recent (Alavi 2007). The Asmari Formation was deposited in such a peripheral foreland (proforeland) system.

Most of the Zagros traps are anticlinal in origin and are in consistent with the NW–SE trend of the Zagros Belt (Murriss 1980), also it is presumed that the migration of hydrocarbon was triggered by the Zagros orogenic movements (Aqrabi et al. 2006). The hydrocarbon accumulation in south, west, and southwest Iran is highly dependent on the stratigraphy and structural evolution of the Zagros range (Alavi 2007).

The Simply Folded Zone as the external part of the Zagros range (Alavi 1980, 1991, 1994) extends for nearly 2,000 km from south eastern Turkey through northern Syria and north eastern Iraq to western and southern Iran (Alavi 2004, 2007). In the Iranian part, it is divided into six major morphotectonic units, namely Lurestan, Dezful Embayment, Izeh, Fars, Bandar-Abbas Hinterland and Abadan Plain that are bounded by major faults (Fig. 2a).

The Asmari Formation was deposited in the Zagros peripheral foreland basin during Oligocene to Miocene. The formation occurs in most parts of Zagros from Lurestan to Coastal Fars, showing significant variation in thickness and facies. The formation obtains its name from

the Asmari Mountain, SE of Masjed-E Suleyman city, where it was studied first (Fig. 1c) and is selected as its type section (Richardson 1924; Thomas 1951).

The Asmari Formation was deposited on a tropical platform, which covered SW Iran (Henson 1951; Dunnington 1958, 1967; James and Wynd 1965). The formation displays a large-scale trend of upward-decreasing accommodation. The lower Asmari strata were deposited in open-marine conditions, reflecting a prograding marginal to slope settings, whereas the middle to upper parts of the formation were deposited in lower energy settings (Aqrabi et al. 2006).

It is believed (Sharland et al. 2004) that the Asmari Formation was deposited in a time slice of the last tectonostratigraphic megasequence of the Arabian Plate that spanned 34 my. It has been ascertained as a sedimentary sequence lying between both unconformities marking the onsets of Red Sea rifting (Beydoun and Sikander 1992) and the first continent–continent collision between Arabia and Eurasia (Beydoun 1993), which are reflected by the present-day topographic surface. This megasequence corresponds to the Zagros foreland basin sedimentary sequence.

Method of study

This study is limited to northwestern part of the Lurestan zone, where significant exposures of the carbonate–evaporite mixed Asmari Formation are observed. After a reconnaissance of the study area, three sections (Zarrin-Abad, Darreh-Shahr, and Abhar) with different facies characteristics have been selected for detailed description of rocks and sampling (Fig. 3). The sections are selected in such a way to encompass the whole area where the Kalhur Member is exposed.

For the facies analysis a detailed observation, description and measurement of the rocks in the sections, including their lithology, thickness, geometry, sedimentary structure, microfossil and macrofossil contents, and their stratal surface structures have been made in the field. Considering lithological variations in the field, a systematic sampling has been carried out with the aim of analysis of lithology, diagenetic features, microfossil contents and geochemical properties of the rocks in the laboratory. To study the nature of the bounding surfaces of the formation, the uppermost part of the underlying Pabdeh Formation and the lowermost part of the overlying Gachsaran Formation (Fig. 1) have been also investigated. Based on the lithofacies analysis in the field, more than 350 samples have been selected for petrographic and microfacies studies and laboratory analysis. All of standard thin-sections prepared from rock samples are stained for the observation of mineralogical composition using Dickson (1965) method.

The classification of the carbonate rocks and their microfacies is based on the methods of Dunham (1962), and Embry and Klovan (1971). Frequency of allochems in each facies, their cement and matrix content are determined using point counting methods (Zuffa 1985).

Facies patterns of the carbonate–evaporite mixed Asmari Formation are identified by lithologic and microfacies analyses. Based on the study of sedimentological characteristics of every facies and on the comparison of the study result with that of standard facies belts of well-known sedimentary environments in the world (Wilson 1975; Buxton and Pedley 1989; Burchette and Wright 1992; Pedley 1998; Pomar 2001; Flügel 2004), the depositional environment of every facies is determined. Facies with comparable sedimentological characteristic (genetically related) are considered as facies association (Miall 2000). On the basis of sedimentological characteristics of facies, the shallowing/deepening-up nature of facies associations, their stratal surfaces of regressive, transgressive, flooding, or erosional horizons, major systems tracts and sequences of the formation are determined. Determination of all major stratal surfaces and systems tracts proposed here follows definitions of Hunt and Tucker (1992, 1995), Tucker et al. (1993) and Tucker (1991).

Stratigraphy

Typically, the Asmari Formation in southwestern Lurestan, where the Kalhur Member is exposed, represents the following units (Adams 1969):

1. Lower Kalhur Gypsum (ca. 3–20 m): this basal unit consists of a series of massive bedded gypsums.
2. Inter-Kalhur Beds (ca. 17–75 m): this unit is composed of a series of well-bedded to shaly bedded green gray marls, and gray marly limestone, which mostly contain pelagic fauna.
3. Upper Kalhur Gypsum: this forms a massive bedded gypsum unit with some rare thin limestones intercalations.
4. Transition Beds (ca. 0–70 m): this unit is composed of thin–medium bedded alternations of dolomitic limestones, marly limestones, marls and gypsums.
5. Upper and Middle Asmari Limestones.

Among the studied sections, only the Zarrin-abad section (south flank of the Anaran anticline) shows the typical succession of the Kalhur Member. At the Abhar section (north flank of the Kabir-kuh anticline) and Darreh-shahr section (south flank of the Kabir-kuh anticline), upper Kalhur gypsum and transition beds are missed, and the sections only show lower Kalhur

gypsum, inter-Kalhur beds, and middle and upper Asmari limestones (Figs. 6, 7, 8).

Facies analysis

In the studied area, 16 facies have been determined. Facies with similar characteristics, which are thought to be genetically related, are grouped as a facies association (named A to E). Each facies association represents specific depositional conditions, the ordering of which is aimed at reconstruction of the depositional environment of the whole formation.

Facies A₁: Hemipelagic bioclast packstone–grainstone

The packstone–grainstone is composed of a variety of allochems in terms of type and size, including mainly sand- to silt-sized fragments of red algae, planktonic and benthic foraminifera (mostly porcelaneous). Echinoderm and bivalve fragments are the accessory constituent. The facies shows storm-induced nature at bottom with erosional lower surface and showing mixed pattern of shallow and deep water allochems (Fig. 3a).

Facies A₂: Planktonic foraminifera wackestone–packstone

Sand-sized biochemes of planktonic foraminifera are the main allochems, which mixed with minor thin-shelled bivalves, echinoderm and ostracod shell fragments in the framework (Fig. 3b). Partly, the facies shows a marly nature due to the abundance of silt- to clay-sized detrital grains (Fig. 3c).

Interpretation: The facies A₁ and A₂ (known as facies association A) are related to the outer ramp setting, based on their sedimentological characteristics and faunal content (cf. Buxton and Pedley 1989; Pedley 1998). Abundant planktonic foraminifera within a micritic matrix indicate the calm and aphotic condition, below storm wave base (SWB). Local occurrence of terrigenous material in some samples indicates periodical effects of storms in this part of the basin (Figs. 6, 7, 8, 10).

Facies B₁: Coralline algae rudstone to packstone

This is a well-known Tertiary facies (Buxton and Pedley 1989; Pedley 1998; Pomar 2001) with significant amount of coralline red algae and porcelaneous benthic foraminifera in the framework. Sand- to gravel-sized fragments of bivalve, bryozoans, oyster (hyaline), echinoderm and peyssonnelid algae are the minor constituents of the

framework (Fig. 3d–g). Rhodoliths are observed in some places (Fig. 3d).

Facies B₂: LBF wackestone

The facies is characterized by a floatstone to wackestone with gravel-sized shell fragments of echinoderm, bivalves, bryozoans, and larger hyaline benthic foraminifera (LBF such as *Operculina* spp.). Sand- to silt-sized quartz grains, along with small benthic and planktonic foraminifera (single-row agglutinated foraminifera and miliolids) and coralline red algae are the minor allochems (Fig. 3h). This LBF-bearing facies is also a well-known Tertiary carbonate platform facies (Buxton and Pedley 1989; Pedley 1998; Geel 2000; Pomar 2001).

Interpretation: The facies B₁ and B₂ (facies association B) characterize the mid-ramp in the studying sections. Abundant coralline red algae rudstone to packstone (facies B₁), as the most prominent facies of the Miocene ramps (Pedley 1998; Pomar 2001), indicates shallow sub-tidal to near oligophotic conditions (Buxton and Pedley 1989; Pedley 1998; Pomar 2001). Common porcelaneous benthic foraminifera in this facies point to the euphotic condition (e.g., Geel 2000). Abundant red algae in the facies have locally produced rhodolith pavement in the deeper part of the zone (i.e., mesophotic zone; Fig. 3d). The facies with larger benthic foraminifera (facies B₂) indicates the oligophotic condition (c.f. Geel 2000; Pomar 2001; Vaziri-Moghaddam et al. 2006) and distal part of the mid-ramp according to Buxton and Pedley (1989). Therefore, this facies association extends from euphotic (sub-tidal) to oligophotic zones and encompasses the mid-ramp of the Asmari sedimentary environment.

Facies C₁: Red algae foraminifera rudstone–grainstone

Red algae detritus and benthic foraminifera (miliolids, *Elphidium* sp., *Peneroplis*, Alveolinidae) are the main components of this facies (Fig. 3i, j). Gastropod, echinoid, calcitic bivalve, *Rotalia* sp., codiacean green algae, bivalve with primary aragonitic shell, bryozoans and intraclast are minor allochems. Micritization of shell fragments is locally observed.

Facies C₂: Oolitic grainstone–packstone

This is a well-sorted facies, in which the main allochems are dominantly superficial ooids. Minor allochems are shell fragments of porcelaneous benthic foraminifera (such as *Meandropsina* sp., miliolids, *Dendritina* sp., *Spirolina* sp., and *Peneroplis* sp.), bivalve, gastropod, oyster, echinoderm, peyssonneliacean algae, coralline red algae, green algae, intraclast and faverina (fecal pellets from a kind of

crustacean). Bioclasts occur as dominantly these of ooid nuclei (Fig. 3k). Carbonate matrix is locally observed, providing a packstone texture for the facies.

Facies C₃: Bioclast rudstone to floatstone

The facies is characterized by pebble-sized oyster fragments along with granule- to sand-sized fragments of red algae, hyaline benthic foraminifera, and echinoids. Red algae are also observed, which locally acts as a binding organism. Bioclasts of gastropod, bivalve, coral, green algae, bryozoans and pellets are the minor constituents (Fig. 3l). The matrix occurs in the form of blocky cement or micrite.

Facies C₄: Coral boundstone

Scleractinia or hexacoral is the main component of this facies that was bounded organically during deposition. The aragonite of the coral's wall was replaced commonly by calcite. Micrite entrapment in coral chambers is commonly observed (Fig. 3m). Some patchy bioherms of the facies are observed in the field. van Buchem et al. (2010) also reported patch-reef bioherms from Dezful Embayment (Kuh-e-Khaviz and Kuh-e-Razi).

Interpretation: Facies association C shows characteristics of various high-energetic sub-environments of the inner ramp setting. The oolitic and bioclastic shoal facies (facies C₁ and C₂), are the most prominent facies of this setting (Fig. 10). They point to the higher energy parts of the inner ramp (around fair weather wave base or FWWB). Some facies of this group (facies C₃ and C₄) indicate the patch-reef region, which seems to be locally developed around the FWWB (cf. Buxton and Pedley Buxton and Pedley 1989; Pedley 1998; Fig. 10).

Facies D₁: Mollusk wackestone–packstone

The facies is characterized by containing abundant mollusk (bivalve and gastropod) shell fragments and miliolids in the framework. Bioclasts of echinoid, coralline red algae, peyssonneliacean red algae, bryozoans, small hyaline benthic foraminifera, green algae, worm tubes, peloids and pellets are minor constituents (Fig. 3n). The matrix content highly varies in the wackestone and packstone. Geopetal fabric is locally observed in some mollusk shells.

Facies D₂: Bioturbated peloidal wackestone–mudstone

Such wackestone–mudstone facies is characterized by being subject to intensive bioturbation. Peloids, porcelaneous benthic foraminifera (often miliolids), scattered

hyaline benthic foraminifera, coralline red algae and echinoderms are the main allochems, but their abundance rarely exceeds 20 % (Fig. 3o). Most of the peloids are of bahamite type (created by micritization of primary allochems).

Facies D₃: Rotalian bioclast wackestone–packstone

This is a wackestone to packstone, in which small rotalids (small benthic hyaline foraminifera) and ostracod shell fragments are the main allochems. *Elphidium* sp. 14,

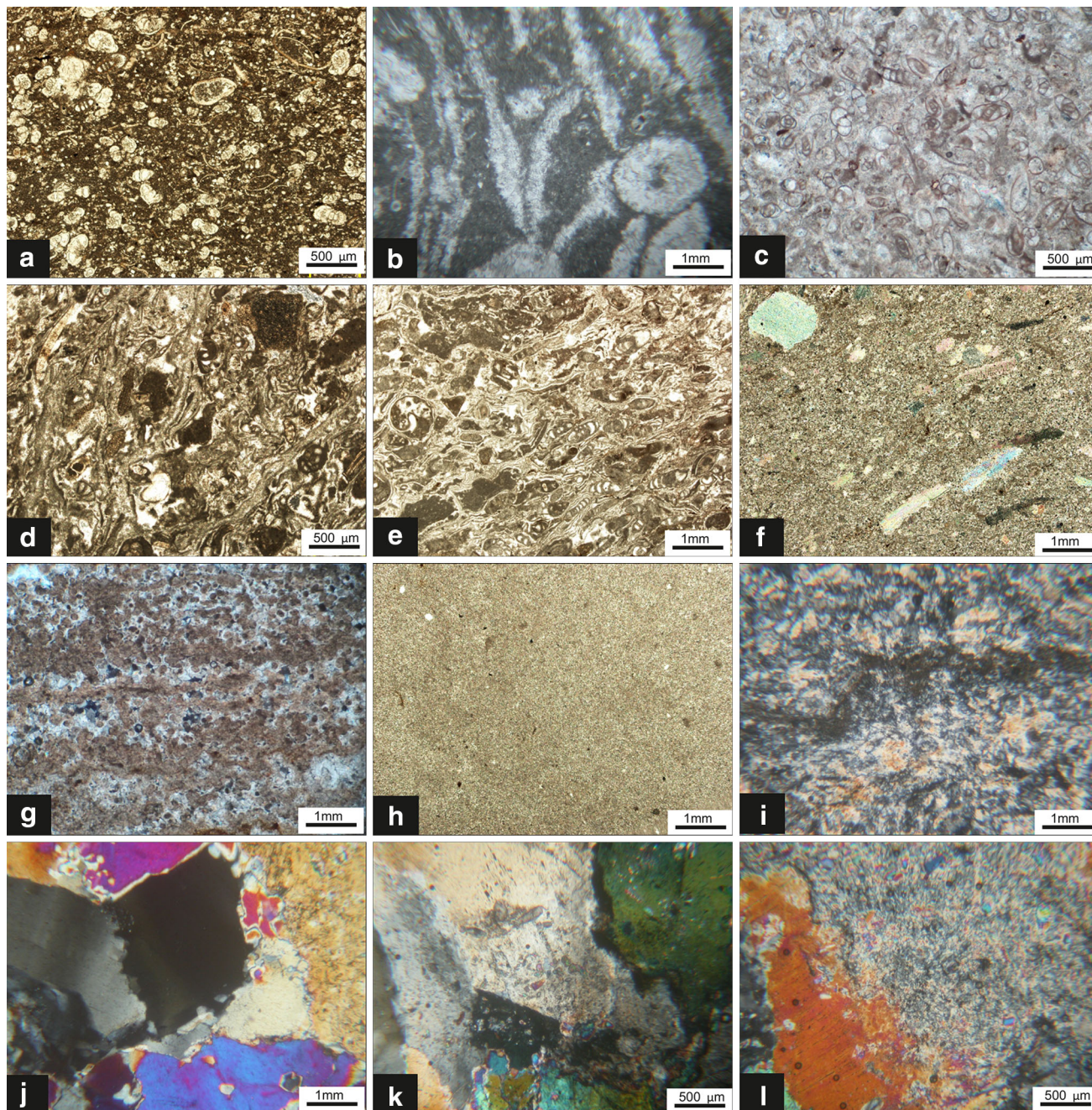
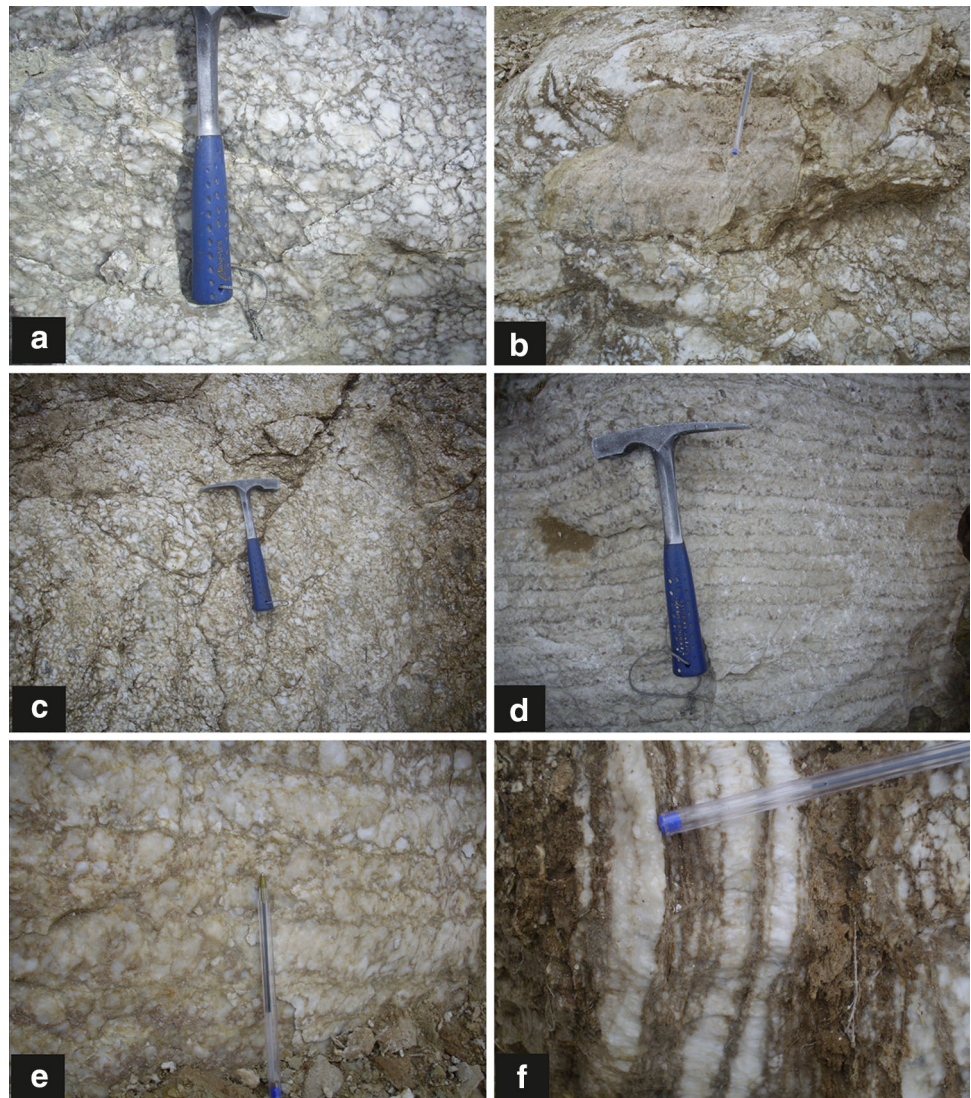


Fig. 4 Representative photomicrographs of some facies in the studied sections: **a** Rotalian bioclast wackestone–packstone (D₃); *Amoina* sp. and *Elphidium* sp. 14 along with minor *Discorbis*, and ostracods make the constituents of the facies. **b** Green algae rudstone to floatstone (D₄). **c–e** Bioclastic wackestone (D₅); miliolida, and other porcelaneous benthic foraminifera are the main allochems.

f Echinoid wackestone (D₆). Facies F; stromatolite boundstone (**g**) and dolo-mudstone (**h**). **i–l** Evaporite facies (E); alabastrine (**i**) and porphyroblastic (**j**, **k**) textures are the common micro-textures of the Kalhur Member evaporites. Modification of the porphyroblastic texture into the alabastrine one is also locally observed (**l**)

Fig. 5 Representative macroscopic (field) views of the facies E (anhydrite) with characteristic brecciated (a–c), elongate nodular (d, e), and satin spar (f) textures



echinoid and calcitic shell fragments of bivalves are minor constituents of the framework. Tiny fragments of ostracods, mostly broken and crushed with sand- to silt-sized fragments of benthic foraminifera occur in the micritic matrix (Fig. 4a).

Facies D₄: green algae rudstone to floatstone

The facies of rudstone to floatstone (Embry and Klovan 1971) is composed of mainly gravel-sized green algae detritus, in which sand- to gravel-sized shell fragments of benthic foraminifera are the minor allochems (Fig. 4b).

Facies D₅: Bioclastic wackestone

Bioclasts of miliolida and other benthic foraminifera (porcelaneous) are the main allochems of this facies. Sand- to gravel-sized fragments of bivalves (aragonitic to

calcitic), echinoids, gastropods, bryozoans and hyaline benthic foraminifera are the minor allochems of the facies. (Fig. 4c–e).

Facies D₆: Echinoid wackestone–floatstone

Gravel-sized shell fragments of echinoids are the main allochems in the facies, which are scattered in micritic matrix. Bioclasts of red algae, bivalve and benthic foraminifera (*Elphidium* sp. 14, and *Rotalia* sp.) are the minor allochems (Fig. 4f). Disaggregation of echinoderm shell fragments into mud size particles (matrix) is widely observed.

Interpretation: The facies association D (facies D₁–D₆) shows characteristics of the restricted lagoon in the inner ramp setting. Micritization, bioturbation, abundant lagoonal biota (such as miliolida, porcelaneous benthic foraminifera, and mollusk shell fragments), peloids and leading

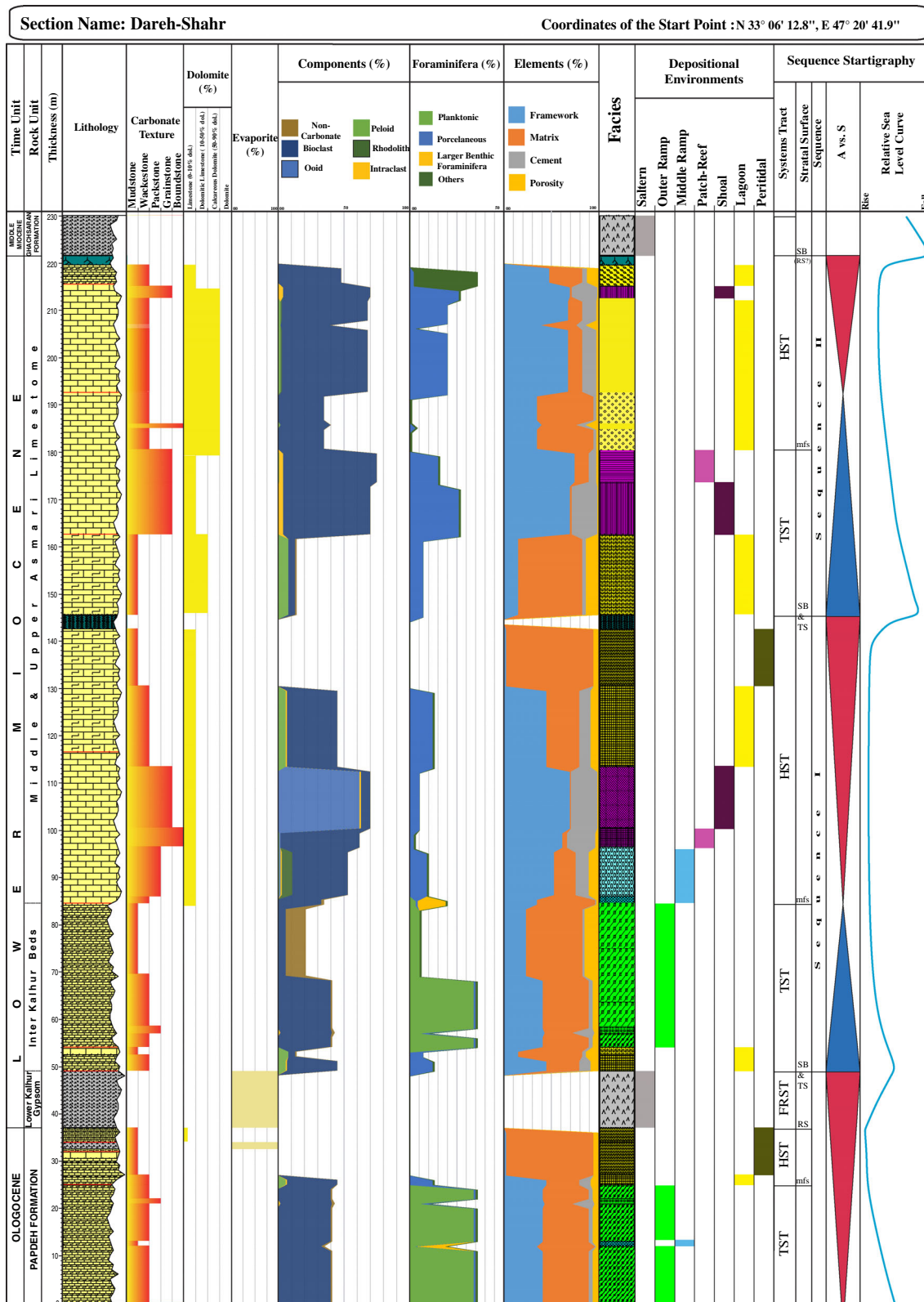
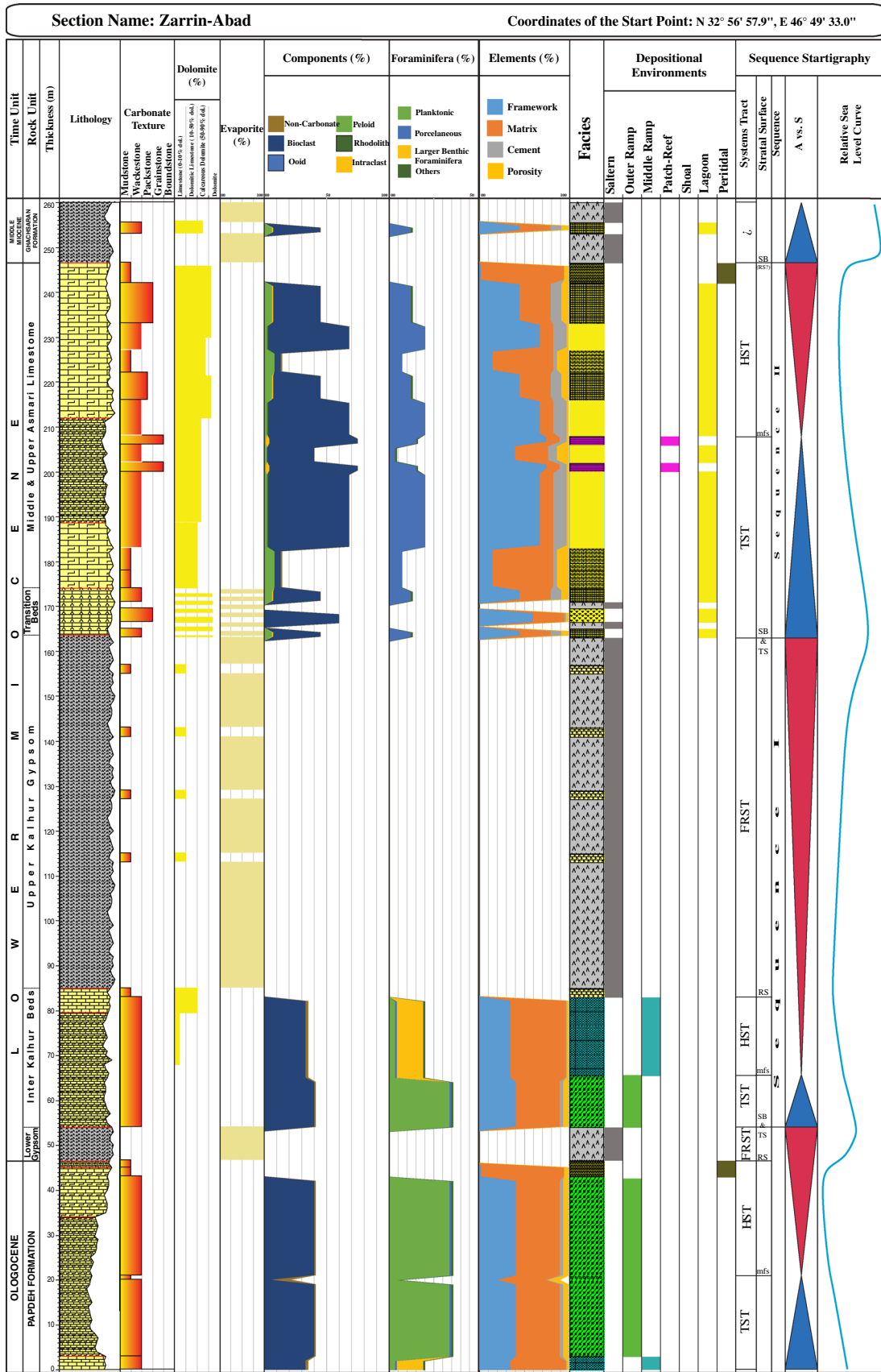


Fig. 7 Sedimentological log of the Asmari Formation in the Darreh-Shahr Section, and its constituent sequences, systems tracts, and strata surfaces. For legend see Fig. 9



◀ **Fig. 8** Sedimentological log of the Asmari Formation in the Zarrin-Abad section, and its constituent sequences, systems tracts, and strata surfaces. For legend see Fig. 9

amount of matrix are the common features of these facies (Buxton and Pedley 1989; Tucker 1991; Tucker and Wright 1990; Flügel 2004; Vaziri-Moghaddam et al. 2006).

Facies E: Anhydrite

The facies association E, known as the Kalhur Member, is dominated by gypsum/anhydrite layers, few millimeters up to meters thick (facies E), with intercalations of delicate and wavy lime mudstone to fecal pellet wackestone, dolomitized mudstone, and marl. These carbonate intercalations are marked by abundant fecal pellets and extensive dolomitization.

In terms of composition, this facies is composed of anhydrite and gypsum with few intercalations of limestone and dolomitic limestone. Anhydrite is the dominant lithology that has been altered to gypsum to some extent. In terms of macro-texture (cf. Warren 2006), the facies dominantly occurs in the form of *brecciated gypsum* (Fig. 5a–c) and *elongate nodular anhydrite* (Fig. 5d, e). The latter is the most dominant and typical texture in the facies. The *satın spar* texture is locally observed in the facies (Fig. 5f). According to the petrographic micro-texture study, some gypsum show *alabastrine* (microcrystalline gypsum with indistinct to semi-distinct boundaries) and *porphyroblastic* (large, idiomorphic crystals (1–5 cm) with distinct boundaries, which may contain abundant remnant of anhydrite laths) textures (Fig. 4i, j, k, respectively). Modification of the porphyroblastic texture into the alabastrine one is locally observed (Fig. 4l).

Interpretation: According to geometry and sedimentation textures of evaporites, the evaporites may reflect and represent three different depositional settings (Warren 2006):

1. Mudflat evaporites (sabkha), generally are composed of successions of stacked, shoaling-upwards, mud matrix dominated units, with limited lateral extension and typical textures like chicken wire, introlithic, nodular textures, and also with extended erosional surfaces.
2. Saltern evaporites with layers of extensive shallow evaporites are deposited across hundreds of kilometers in the hypersaline portions of an ancient evaporite environment (Warren 1991). Despite previous group, the successions made by these evaporites tend to have more purity and no/low matrix. The most typical textures among these evaporites are *growth-aligned gypsum* and *elongate nodular anhydrite*.

3. Deep water evaporates are known as evaporites deposited in deep waters with striking *laminar texture*.

With regard to the existence of the marked *elongate nodular anhydrite* texture, characterizing saltern setting, and vast lateral extension of these evaporites in the area, they may represent a saltern environment.

Facies F: Limemudstone

The carbonate mudstone is characterized by a laminar structure, or cryptalgal fenestral fabrics (Fig. 4g, h). Obvious stromatolitic texture was also observed in some places (Fig. 4g). Evaporite crystals may be common. Dolomitization is a prevalent feature in this facies. The facies is locally marked by bioturbation. Silt-sized quartz grains are also locally observed, in abundance of which there produces a mixed nature of them with other components in the facies.

Interpretation: Blue–green algae, microbial fabrics, evaporite mineralization and fenestral fabric are all the evidences that confine peritidal setting for this facies (Wilson 1975; Tucker and Wright 1990; Flügel 2004).

Distribution of the described facies in the three studied sections can be seen in Figs 6, 7, 8, 9.

Depositional environment

The findings of depositional conditions of the facies associations show that the Asmari Formation in the studied sections was deposited on a carbonate ramp, which was connected with an intrashelf basin (Figs. 10, 11). The lack of significant reefal and reef-talus facies, the transitional change of the facies characteristics in time and space, the significant amount of red algae in the carbonate facies, and the abundance of evaporites (Kalhur Member) support the understanding of these settings (cf. Tucker 1991; Burchette and Wright 1992; Pomar 2001; Flügel 2004; Warren 2006).

Precipitation of widespread marine seepage-fed platform evaporites requires the hydrological stability associated with much gentler sea-level fluctuations (greenhouse earth climate). Also they need a sizeable area on the earth surface where the appropriate combination of tectonics and climate would lead to *hydrographically isolated* and dissected basin (Warren 2006). Deposition of the carbonates along with the evaporites points to the fact that the evaporite deposition has had a periodic event and this requires proper combination of tectonic setting, sea-level fluctuations and climatic condition. The best explanation for this alternation is a tectonically driven intrashelf basin (Tucker 1991; Burchette and Wright 1992; Warren 2006), which in response to sea-level fluctuations is periodically dissected

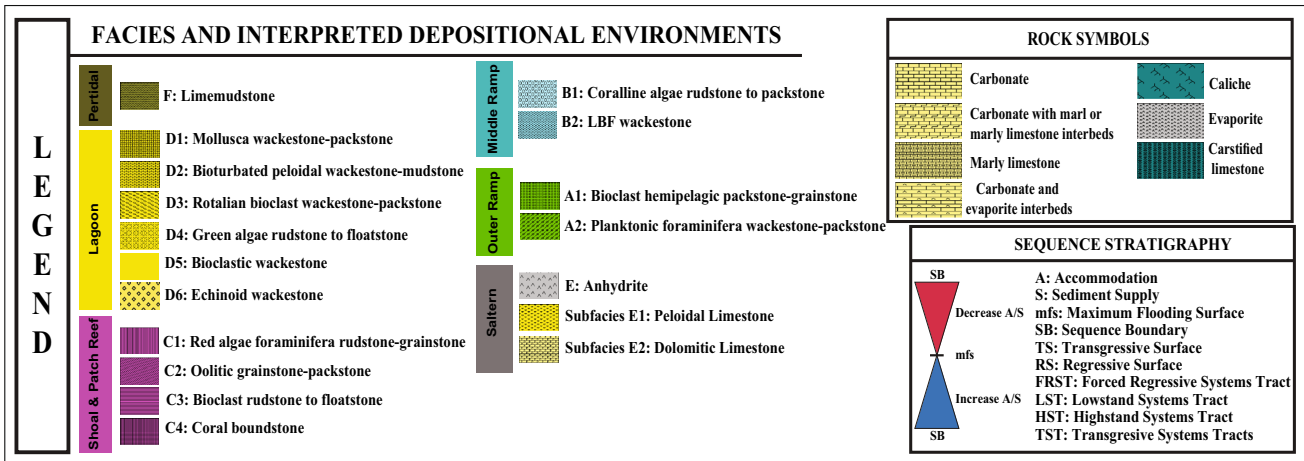


Fig. 9 Legend for some illustrations used in this paper

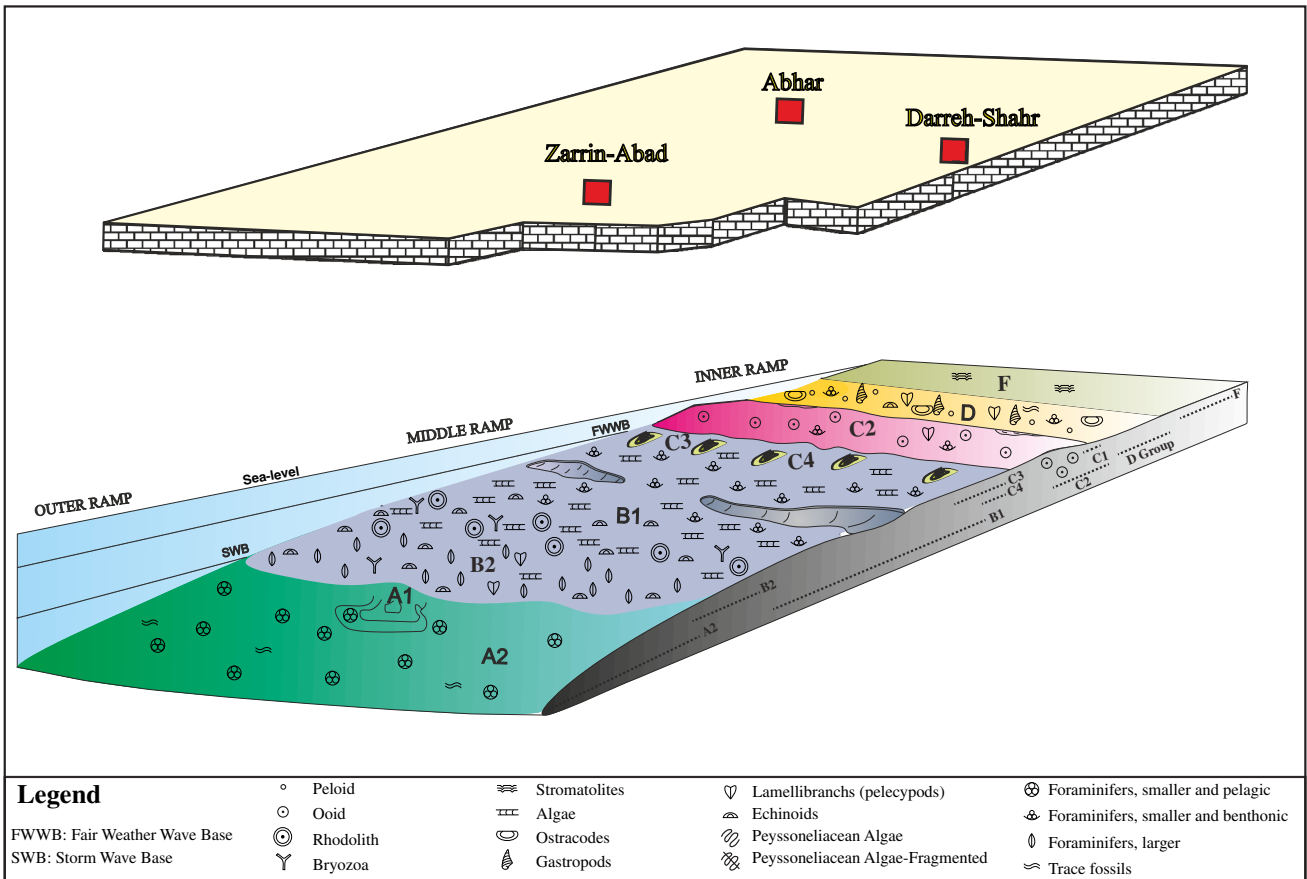


Fig. 10 Depositional model of the Asmari Formation in the studied sections (after Buchette and Wright Burchette and Wright 1992). Note the model only illustrates deposition of the carbonate rocks, for

understanding the evolution of the carbonate–evaporite mixed Asmari basin through time (dynamic depositional model) see Fig. 11

from and reconnected to open sea and in conjunction with arid climatic condition led to a periodic carbonate-evaporite basin (Fig. 11).

In such intrashelf basin, during sea-level rises, connection of the intrashelf to the rest of the Zagros foreland basin (SE Zagros) was possible and thus carbonate strata were

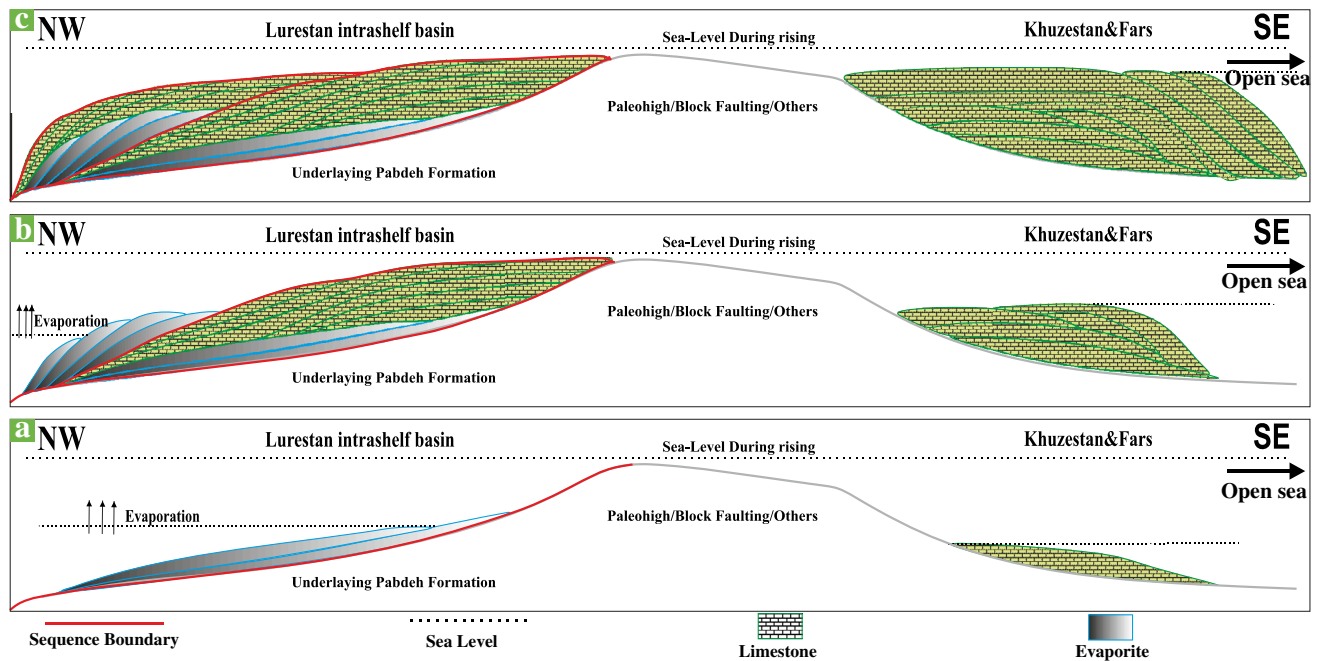


Fig. 11 Evolution of the Asmari basin through time. While the deposition was probably continuous in SE (the Khuzestan and Fars regions), the Lurestan region was subjected to a periodically hydrographic isolated basin in which evaporites were deposited during sea-level falls and carbonates during risings of sea level. **a** Deposition of the basal anhydrite (Figs. 6, 7, 8) across the region during the first sea-level falling stage. **b** Deposition of the upper unit

of evaporites (known as the upper Kalhur gypsum, only seen in the Zarrin-abad section) during the second sea-level falling. Before this phase of evaporite precipitation, a sea-level rising resulted in deposition of the carbonates (Fig. 10). **c** Deposition of the carbonates on the underlying evaporites or exposed carbonates during sea-level rise. These cycles led to two probably second-order sequences in the studied area

deposited. On the other hand, sea-level falls resulted in the basin restriction and evaporates were deposited alternately (Fig. 11).

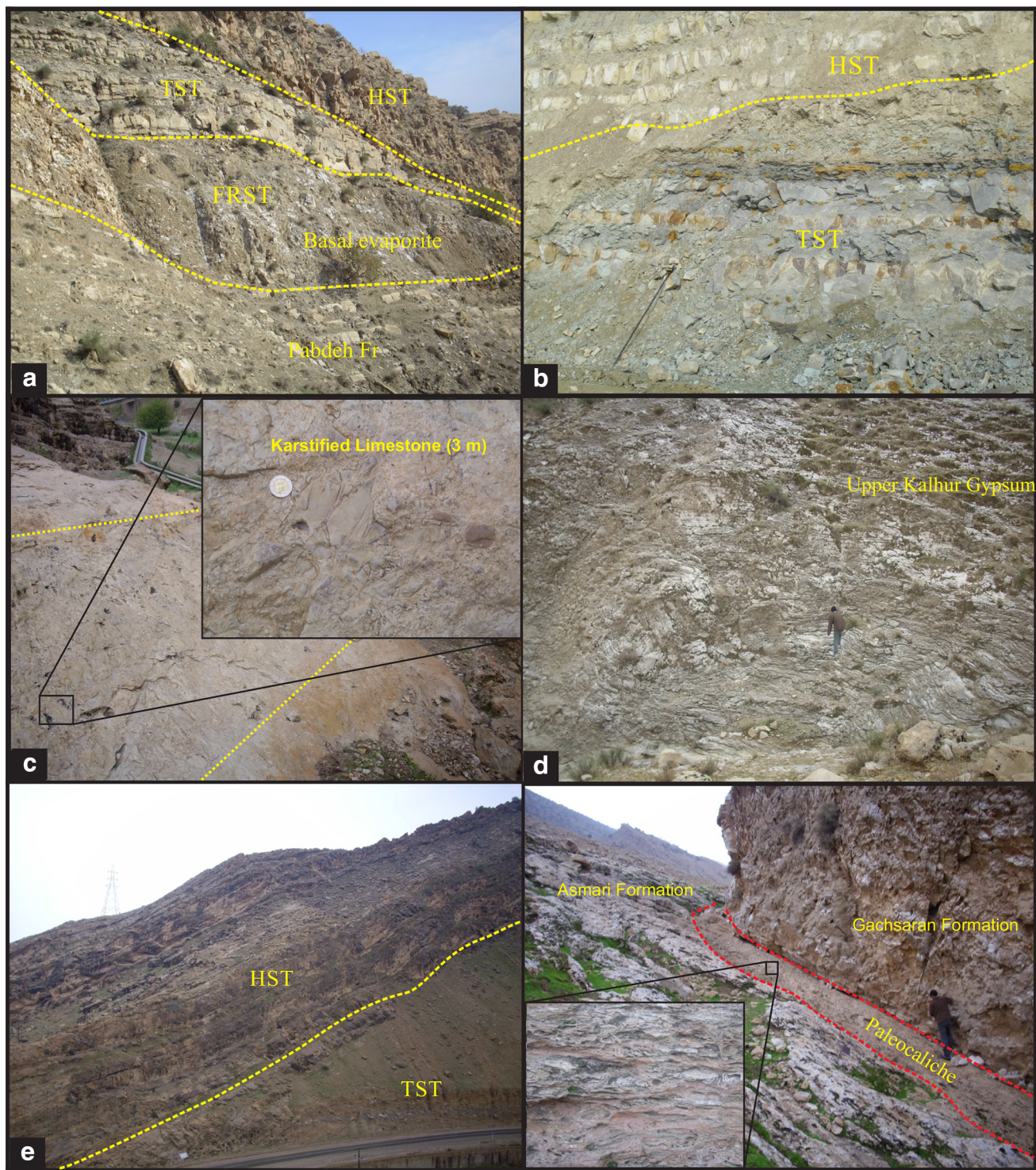
Some authors in recent years have noted this type of basin, in which there developed the Oligo-Miocene deposits of the Zagros foreland basin (e.g., Bahroudi and Koyi 2004; Heydari 2008; Kavooosi and Sherkati 2012). Alavi (2007) believes that the Kalhur Member was deposited in the back-bulge depocenter of the Zagros proforeland basin. Such depressions (either intrashelf or back-bulge) were mostly capable of evaporite development during relative sea-level fall stages and subsequent basin restriction (cf. Shearman and Fuller 1969; Warren and Kendall 1985; Tucker 1991; Warren 1982, 1991; Kendall 1992; Fig. 11).

Sequence stratigraphy

The sequence stratigraphic analysis of the formation is mainly based on facies characteristics and the nature of stratal surfaces. The study result of lithofacies and microfacies analyses is also used for this purpose (Figs. 6, 7, 8).

The Asmari Formation is with a basal of evaporates in the thickness of a few meters (Lower Kalhur Gypsum;

Figs. 6, 7, 8), which follows the strata of deep-marine sediments of the underlying Pabdeh Formation (Fig. 12a). The evaporites display that the basin became restricted and therefore the deposits of this interval belong to the falling-stage systems tract (FSST). Outer ramp deposits (inter-Kalhur beds; Figs. 6, 7, 8) upon this evaporite unit (Fig. 12a) show abrupt rising in sea level and thus pertain to transgressive systems tract (TST). This systems tract in the Zarrin-abad Section ends to a marked zone, which is composed of ferruginous nodules and hardground surfaces (Fig. 12b) and hence it can be regarded as a maximum flooding surface/zone (mfs). The strata character of all the three sections shows that the rapid sea-level rising inclined and deeper paleo-environments give rise to the shallower deposits of the middle ramp (Facies B1). Shoaling-upward conditions can be observed in the Abhar and Darreh-shahr sections, which show obviously the lagoon to peritidal transition. The Zarrin-abad section does not show this transition, which may be located in the deeper position with less sediment accretion. Upward along the sedimentary sequence, the two proximal sections of Abhar and Darreh-shahr show evidences of subaerial exposure indicated by the paleokarst horizons (Fig. 12c). The Zarrin-abad section, overlying the horizon deposited on the mid-



ramp (Facies B1) shows a thick evaporite unit known as the upper Kalhur gypsum (Figs. 8, 12d). According to the mentioned description, the shallowing-upward carbonate unit corresponds to highstand systems tract (HST) and the evaporites of the Zarrin-abad section to the FSST, and the

subaerial exposure surface are correlated with the evaporites (Fig. 13). With the advent of marine regression and sea-level lowering, most part of the basin was led to subaerial exposure, the deposition center was shifted to the deepest part of the basin, and the basal restriction led to

Fig. 12 Some sequence stratigraphic elements of the studied area. **a** Basal anhydrite of the Asmari Formation and the main systems tracts of the first sequence of the formation in the Darreh-shahr section. **b** Maximum flooding surface at the contact of the TST and HST of the first sequence, Zarrin-abad section. Yellow-colored ferruginous nodules and hardground features can be observed in this section. **c** Subaerial exposure surface with extensive karstification and brecciation makes the top of the first sequence in the Darreh-shahr section. **d** A view displaying part of the Kalhur Member (Upper Kalhur Gypsum). This gypsum unit is only seen in the Zarrin-abad section. **e** The TST and HST of the last sequence of the formation, Darreh-shahr section. **f** Paleocaliche horizon at the contact of the Asmari Formation with overlying Gachsaran Formation in the Darreh-shahr section. Irregular laminated crusts and nodular carbonates are the main evidences of a paleocaliche profile (James and Choquette 1984), which can be seen. This surface makes the SB of the sequence

the accretion of the evaporites. The subaerial surfaces or the top of the evaporites can therefore be regarded as sequence boundary (SB). The succession between the basal evaporite and this SB represents the first sequence of the Asmari Formation in the studied area (Figs. 6, 7, 8).

The second sequence of the formation begins with a deepening-upward succession, which can be assigned to the TST (Figs. 6, 7, 8). The final part of the Asmari Formation represents a succession of lagoon-dominated deposits that show more or less aggradational stacking pattern (Fig. 12e), and the Darreh-shahr section terminates to a paleosol horizon (Fig. 12f). This horizon and comparable surfaces in the other section (the contact of the Asmari and Gachsaran formations) is the SB of the second sequence. So the strata can be considered as the HST. In general, the second sequence of the formation contains more shallow-water facies, which show successive shallowing of the basin. Such a large-scale trend of upward decreasing in accommodation space has been reported in the Asmari reservoirs of SW Iran (e.g., Aqrabi et al. 2006; Ehrenberg et al. 2007; Mosadegh et al. 2009). The fact of successive shallowing was the result of the consecutive closure of the Zagros proforeland basin (Alavi 2004).

Discussion

The dynamic depositional model of the intrashelf basins in the sequence stratigraphy framework has been explained by Tucker (1991). While an intrashelf basin is fully connected with the world ocean (i.e., the sea level is above barrier height), carbonate platforms will occur around the basin. In this stage, flooding of a basin results in the development of a retrogradational TST, followed by the aggradational–progradational HST in shallow-water carbonates (Fig. 13). Where sea-level falls close to or just below the barrier

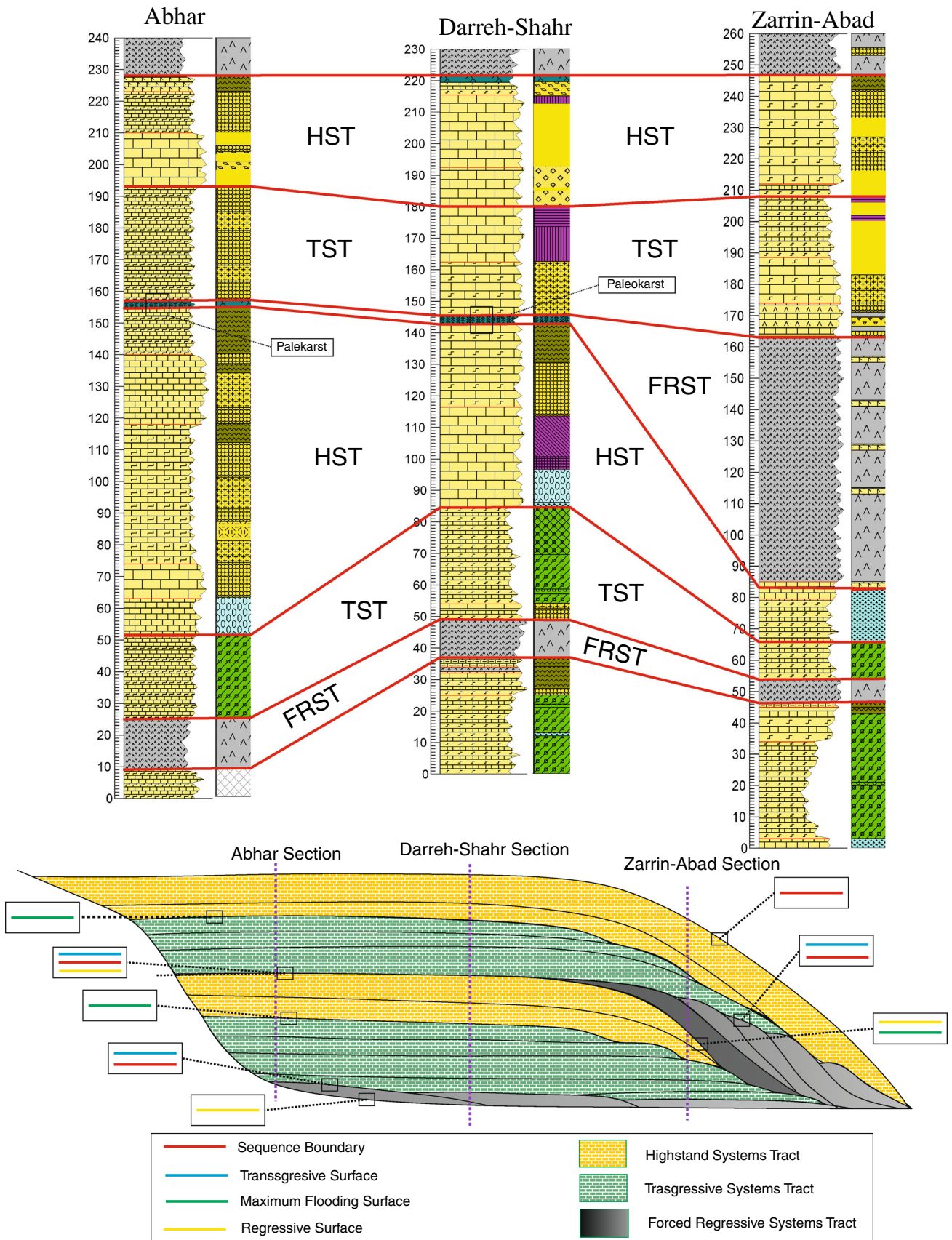
height, through a eustatic fall or tectonic movement of the barrier, the water level within the basin will quickly fall below the shelf break of the marginal carbonate platforms (Fig. 11). Under an arid climate, water within the basin will rapidly become hypersaline, and gypsum will precipitate in abundance around the basin margins, and below the carbonate platform margins, to form wedges (Fig. 12). The base of the evaporites represents the start of relative sea-level fall (regressive surface). The gypsum will be deposited in sabkhas but particularly in shallow hypersaline waters (saltern) to build up a falling-stage wedge (Fig. 13). Resedimentation of the gypsum into deeper water by storms, slope failure, debris flows and turbidity currents will give graded beds, slumps and breccias (Fig. 5a–c). During the falling stage (FRST) and evaporite precipitation, the carbonate platforms will be exposed and may be subjected to subaerial erosion, karstification and dolomitization (the Abhar and Darreh-shahr sections in Fig. 13).

In this regard, a relative sea-level fall was recorded in the Zarrin-Abad Section by widespread development of the facies association E (the upper Kalhur gypsum; Fig. 8). Accordingly, the Kalhur Member in the Zarrin-Abad section represents the falling-stage systems tract wedges (FRST) of a second-order sequence, the relative sea-level fall is recorded as paleocast horizons in the other two sections (Figs. 6, 7, 8, 13), illustrating a major exposure in these parts of the basin. The correlation clearly shows the deeper condition of the Asmari basin in the Zarrin-Abad Section, where the basin is not significantly affected by the second-order sea-level fluctuations (Fig. 13). When the basin is reconnected with the open ocean, the formerly exposed carbonate platforms will be flooded and the TST, and then HST will be established (Fig. 13).

Considering the constituent sequences (Figs. 6, 7, 8) of the Asmari Formation and its under- and overlying strata of Pabdeh and Gachsaran Formations, the Asmari Formation shows a regressive trend, during which the deep-marine facies of the Pabdeh Formation was transitionally changed to shallow-water-evaporitic and continental facies of the Gachsaran Formation. Such a trend finally resulted in the filling and closure of the Zagros proforeland basin.

Conclusions

1. The studied sections of the Asmari Formation show greater variety of facies such as carbonate, evaporitic and mixed ones than that in other parts of the Zagros belt. This is mostly due to its periodical appearance of restricted depositional condition, compared to that in other parts of the Zagros proforeland basin. The periodical change of paleo-environments resulted in the depositional alternation of carbonates and



◀ **Fig. 13** Sequence stratigraphic correlation and model of the Asmari Formation in the studied sections. Dominance of the lagoonal facies in the Abhar section, and the high-energy ramp margin facies in the Dareh-Shahr section point their deposition in the landward portion of the basin. Precipitation of thick evaporites in the Zarrin-abad section, which are comparable to the subaerial exposure features of the other two sections suggesting its deposition in distal portion of the basin. Evaporites of the Zarrin-abad and the basal anhydrite are related to the sea-level falling-stage systems tract (FSST or FRST). In the model, some stratigraphic surfaces are superimposed

evaporites. The abundance of evaporites in the formation characterizes the environment of hydrographically isolated basin.

2. The facies change through time and space along the column of Asmari Formation occurred in the intrashelf basin, which can explain the diversity of rock characters of the formation. Dissecting of the basin during sea-level falls is the reason why alternation of evaporite with carbonate deposits occurred.
3. The variety of the facies through time was originally controlled by the paleo-tectonics of the basin, arid climate condition and relative sea-level changes on a medium scale (probably second-order).
4. The Zarrin-Abad section is located in an outstanding place in the region, in which the falling-stage systems tract is recorded as a sediment package of evaporites, represented by the upper Kalhur gypsum.
5. The facies of Asmari Formation represent a regressive trend in the intrashelf basin, which reflect a transitional condition from deep-marine setting (represented by its underlying Pabdeh Formation) to continental setting (represented by its overlying Gachsaran Formation).

Acknowledgments The University of Tehran provided facilities for this research, for which the authors are grateful. This study was financially supported by Iranian Central Oil Field Co (ICOFC). The authors would like to acknowledge the company for the support and permission to publish these results. Some data for this study is provided by H. Mohammadpour. Special thanks are expressed to M. Lankarani and M. R Tabarzadi for their help in the field studies and preparation of photographs, respectively. Esfandiar Mohammadpour is acknowledged for careful driving during the field studies.

References

- Adams TD (1969) The Asmari Formation of Lurestan and Khuzestan Provinces. Rep. # 1154, National Iranian Oil Company internal report (Unpub.)
- Adams TD, Bourgeois F (1967) Asmari biostratigraphy. Geol. Explor. Div, IOOC Rep. # 1024, Tehran, National Iranian Oil Company internal report (Unpub.)
- Ahr WM (2008) Geology of carbonate reservoirs: the identification, description, and characterization of hydrocarbon reservoirs in carbonate rocks. Wiley, Hoboken, New Jersey/Canada
- Ala MA (1982) Chronology of trap formation and migration of hydrocarbons in Zagros sector of southwest Iran. AAPG Bull 66:1535–1541
- Alavi M (1980) Tectonostratigraphic evolution of the Zagrosides of Iran. *Geology* 8:144–149
- Alavi M (1991) Tectonic map of the Middle East: Tehran, Geological Survey of Iran, Scale: 1: 5,000,000
- Alavi M (1994) Tectonics of the Zagros orogenic belt of Iran: new data and interpretations. *Tectonophysics* 229:211–238
- Alavi M (2004) Regional stratigraphy of the Zagros fold-thrust belt of Iran and its proforeland evolution. *Am J Sci* 304:1–20
- Alavi M (2007) Structures of the Zagros fold-thrust belt in Iran. *Am J Sci* 307:1064–1095
- Amirshahkarami M, Vaziri-Moghaddam H, Taheri A (2007) Paleoenvironmental model and sequence stratigraphy of the Asmari Formation in southwest Iran. *Hist Biol* 19(2):173–183
- Aqrabi AAM, Keramati M, Ehrenberg SN, Pickard N, Moallemi A, Svana T, Darke G, Dickson JAD, Oxtoby NH (2006) The origin of dolomite in the Asmari Formation (Oligocene–Lower Miocene), Dezful Embayment, SW Iran. *J Pet Geol* 29:381–402
- Bahrami H (2000) Biostratigraphy and micropaleontological studies on the cutting samples of Changuleh well, north Dezful. Technical Report 1130. NIOCEXP Office Tehran (Unpub.)
- Bahroudi A, Koyi HA (2004) Tectono-sedimentary framework of the Gachsaran Formation in the Zagros Foreland Basin. *Mar Pet Geol* 21:1295–1310
- Berberian M, King GCP (1981) Towards a paleogeography and tectonic evolution of Iran. *Can J Earth Sci* 18:210–265
- Beydoun ZR (1993) Evolution of the northeastern Arabian plate margin and shelf, hydrocarbon habitat and conceptual future potential. *Revue de l'Institut Français du Pétrole* 48:311–345
- Beydoun ZR, Sikander AH (1992) The Red Sea- Gulf of Aden: reassessment of hydrocarbon potential. *Mar Pet Geol* 9:475–485
- Burchette TP, Wright VP (1992) Carbonate ramp depositional systems. *Sed Geol* 79:3–57
- Buxton MWN, Pedley HM (1989) A standardized model for Tethyan Tertiary carbonates ramps. *J Geol Soc* 146:746–748
- Dickson JAD (1965) A modified staining technique for carbonate in thin section. *Nature* 205:587
- Dunham RJ (1962) Classification of carbonate rocks according to their depositional texture. In: Ham WE (ed) Classification of carbonate rocks, vol 1. AAPG Memoir, Tulsa, pp 108–121
- Dunnington HV (1958) Generation, migration, accumulation and dissipation of oil in northern Iraq. *Habitat of Oil*, pp 1194–1251
- Dunnington HV (1967) Stratigraphic distribution of oilfields in the Iraq-Iran- Arabia Basin. *J Inst Pet* 53:129–161
- Ehrenberg SN, Pickard NAH, Laursen GV, Monibi S, Mossadegh ZK, Svana T, Aqrabi AAM, McArthur JM, Thirlwall MF (2007) Strontium isotope stratigraphy of the Asmari Formation (Oligocene–Lower Miocene), SW Iran. *J Pet Geol* 30:107–128
- Embry AF, Klovan JE (1971) A Late Devonian reef tract on northeastern Banks Island. N.W.T. *Bull Can Pet Geol* 19:730–781
- Falcon NL (1958) Position of oilfields in South West Iran with respect to relevant sedimentary basins. In: Weeks LG (ed) *Habitat of Oil*, American Association of Petroleum Geologists Symposium, pp 1252–1278
- Flügel E (2004) *Microfacies analysis of limestones: analysis, interpretation and application*. Springer, Berlin
- Geel T (2000) Recognition of stratigraphic sequences in carbonate platform and slope deposits, empirical models based on microfacies analysis of Paleocene deposits in southeastern Spain. *Palaeogeogr Palaeoclimatol Palaeoecol* 155:211–238
- Ghazban F (2007) *Petroleum geology of the Persian Gulf*. Tehran University and National Iranian Oil Company, Tehran, Iran
- Henson FRS (1951) Observations on the geology and petroleum occurrences of the Middle East. In: *Proceedings of the 3rd World Petroleum Congress*, vol 1, pp 118–140

- Heydari E (2008) Tectonics versus eustatic control on super sequences of the Zagros Mountains of Iran. *Tectonophysics* 451:56–70
- Hunt D, Tucker ME (1992) Stranded parasequences and the forced regressive wedge systems tract: deposition during base level fall. *Sed Geol* 81:1–9
- Hunt D, Tucker ME (1995) Stranded parasequences and the forced regressive wedge systems tract: deposition during base level fall—reply. *Sed Geol* 95:147–160
- IOR (2006) Reservoir description of the Asmari Formation in the Dezful Embayment. National Iranian Oil Company internal report (unpublished)
- James NP, Choquette PW (1984) Diagenesis 9. Limestones—the meteoric diagenetic environment. *Geosci Can* 11:161–194
- James GA, Wynd JG (1965) Stratigraphic nomenclature of Iranian oil consortium agreement area. *AAPG Bull* 49:2182–2245
- Kashfi MS (1984) A source bed study of the Oligo-Miocene Asmari Limestone in SW Iran. *J Pet Geol* 7(4):419–428
- Kavoosi MA, Sherkati Sh (2012) Depositional environments of the Kalhur Member evaporites and tectonosedimentary evolution of the Zagros fold-thrust belt during Early Miocene in south westernmost of Iran. *Carbonates Evaporites* 27:55–69
- Kendall AC (1992) Evaporites. In: Walker RG, James NP (eds) *Facies models: response to sea level changes*. Geological Association of Canada, Newfoundland
- Koop WJ, Stoneley R (1982) Subsidence history of the Middle East Zagros Basin, Permian to Recent. *Philos Trans R Soc Lond* 305:149–168
- McQuillan H (1974) Fracture patterns on Kuh-e-Asmari anticline, southwest Iran. *AAPG Bull* 58:236–246
- Miall AD (2000) *Principles of sedimentary basin analysis*, 3rd edn. Springer, Berlin
- Mosadegh ZK, Haig DW, Allan T, Adabi MH, Sadeghi A (2009) Salinity changes during Late Oligocene to Early Miocene Asmari Formation deposition, The Zagros Mountains, Iran. *Palaeogeogr Palaeoclimatol Palaeoecol* 272:17–36
- Motiei H (1993) *Stratigraphy of Zagros*. Treatise on the Geology of Iran No. 1, Ministry of Mines and Metals. Geological Survey of Iran, Tehran (In Persian)
- Murris RJ (1980) Middle East: stratigraphic evolution and oil habitat. *AAPG Bull* 64:597–618
- Nayebi Z (2003) Biostratigraphy and micropaleontological studies on the cutting samples of Dalpari well, north Dezful. Paleontological note 580. NIOCEXP Office Tehran (Unpub.)
- Pedley M (1998) A review of sediment distributions and processes in Oligo-Miocene ramps of southern Italy and Malta (Mediterranean divide). *Geol Soc Lond Spec Publ* 149:163–179
- Pomar L (2001) Types of carbonate platforms: a genetic approach. *Basin Res* 13:313–334
- Richardson RK (1924) The geology and oil measures of southwest Persia. *J Inst Pet Technol* 10:256–283
- Sadeghi R, Vaziri-Moghaddam H, Taheri A (2009) Biostratigraphy and paleoecology of the Oligo-Miocene succession in Fars and Khuzestan areas (Zagros Basin, SW Iran). *Hist Biol* 20:1–15
- Seyrafian A (2000) Microfacies and depositional environments of the Asmari Formation, at Dehdes area (A correlation across Central Zagros Basin). *Carbonates Evaporites* 15:22–48
- Seyrafian A, Mojikhalifeh AR (2005) Biostratigraphy of the Late Paleogene-Early Neogene succession, north-central border of Persian Gulf, Iran. *Carbonates Evaporites* 20(1):91–97
- Seyrafian A, Arzani N, Taheri A, Vaziri H, Hasheme M (2007) Facies analysis of Asmari Formation in the West/Northwest Zagros Heights. National Iranian Oil Company, internal report (Unpub.)
- Sharland PR, Casey DM, Davies RB, Simmons MD, Sutcliffe OE (2004) Arabian Plate sequence stratigraphy. *GeoArabia*, vol 9, pp 121–124
- Shearman DJ, Fuller JG (1969) Anhydrite diagenesis, calcitization, and organic laminites, Winnipegosis Formation, Middle Devonian, Saskatchewan. *Bull Can Pet Geol* 17(4):496
- Stocklin J (1974) A-Northern Iran: Alborz Mountains, Mesozoic–Cenozoic orogenic Belt, data for orogenic studies. *Geol Soc Lond Spec Publ* 4:213–234
- Takin M (1972) Iranian geology and continental drift in the Middle East. *Nature* 235:147–150
- Thomas AN (1951) The Asmari Limestone of southwest Iran. National Iranian Oil Company internal Report 706 (unpublished)
- Thomas AN (1952) Facies variations in the Asmari Formation. Report of the 18th International Geological Congress (Great Britain), Part 10: 74–82
- Tucker ME (1991) Sequence stratigraphy of carbonate–evaporite basins: models and application to the Upper Permian (Zechstein) of northeast England and adjoining North Sea. *J Geol Soc Lond* 148:1019–1036
- Tucker ME, Wright VP (1990) *Carbonate sedimentology*. Blackwell Scientific Publications, Oxford
- Tucker ME, Calvet F, Hunt D (1993) Sequence stratigraphy of carbonate ramps: systems tracts, models and application to the Muschelkalk carbonate platforms of eastern Spain. In: Posamentier HW, Summerhayes CP, Haq BU, Allen GP (eds) *Sequence Stratigraphy and Facies Associations*. International Association of Sedimentologists, Special Publications, vol 18, pp 397–415
- van Buchem FSP, Allan TL, Laursen GV, Lotfpour M, Moallemi A, Monibi S, Motiei H, Pickard NAH, Tahmasbi AR, Vedrenne V, Vincent B (2010) Regional stratigraphic architecture and reservoir types of the Oligo-Miocene deposits in the Dezful Embayment (Asmari and Pabdeh Formations) SW Iran. *Geol Soc Lond Spec Publ* 329(1):219–263
- Vaziri-Moghaddam H, Kimiagari M, Taheri A (2006) Depositional environment and sequence stratigraphy of the Oligocene-Miocene Asmari Formation in SW Iran, Lali Area. *Facies* 52:41–51
- Warren JK (1982) The hydrological setting, occurrence and significance of gypsum in late Quaternary salt lakes in South Australia. *Sedimentology* 29:609–637
- Warren JK (1991) Sulfate-dominated sea-marginal and platform evaporative settings: sabkha and salina, mudflats and salterns. In: Melvin JL (ed) *Evaporites, Petroleum and Mineral Resources*. Developments in Sedimentology, vol 50. Elsevier, Amsterdam, pp 69–188
- Warren JK (2006) *Evaporites: sediments, resources and hydrocarbons*. Springer, Berlin
- Warren JK, Kendall GC (1985) Comparison of marine sabkha (sub aerial) and salina (subaqueous) evaporites: modern and ancient. *AAPG Bull* 69:1013–1023
- Wells AJ (1967) Lithofacies and geological history of Lower Tertiary sediments in southwest Iran. IOOC, geological report # 1108
- Wilson JL (1975) *Carbonate facies in geological history*. Springer, Berlin
- Wynd J (1965) Biofacies of Iranian Oil Consortium Agreement Area. IOOC Report 1082 (Unpub.)
- Zuffa GG (1985) Optical analyses of arenites: influence of methodology on compositional results. In: Zuffa GG (ed) *Provenance of arenites*. NATO-ASI, Series 148, D. Reidel, Dordrecht: 165–189